arrives at the following equation for ε:

$$C_1 D_{22}^{T} \sin\psi_{22}^{T} = k_2 \sin\varepsilon + C_1 D_{22}^{A} \sin(\psi_{22}^{A} + \delta) - C_2 \sin\varepsilon + C_3 E_{22}^{air} \sin(\Upsilon_{22}^{air} + \delta) \quad (2)$$

where $C_1 = 3\rho_w(1+k_2')/(5\rho_e\bar{H}) = 0.9590\,\mathrm{m}^{-1}$, $C_2 = 3\rho_w h_2(1+k_2')/(5\rho_e) = 4.752 \times 10^{-2}$, and $C_3 = 3(1+k_2')/(5g\rho_e\bar{H}) = 9.445 \times 10^{-5}\,\mathrm{Pa}^{-1}$; k_2 and k_2' are the potential Love and loading numbers (constants that describe how Φ^S depends on the Earth tide and on Earth loading[12]), h_2 the displacement Love number (describing the vertical displacement of the Earth tide[12]), ρ_w and ρ_e are the densities of sea water and Earth, g the gravitational acceleration, and $\bar{H}$ for M_2 equals 8.137 cm. D_{22}^{A}, ψ_{22}^{A} are the coefficients of the altimeter-derived ocean tide (which were derived assuming that $\varepsilon = 0$ and therefore required the small C_2 correction term), and E_{22}^{air}, Υ_{22}^{air} are the coefficients of the lunar barometric tide[21,22]. Angle δ represents an additional phase offset in the ocean plus load tide and the air plus load tide, induced by anelastic response to Earth loading. Because equation (2) is fairly insensitive to δ, we hereafter set it to zero. (If δ were as large as 1°, its neglect would affect the estimated ε by only 0.07°. Further, there is no physical reason to expect that $\delta \gg \varepsilon$; theoretical calculations based on various Earth models[23,24] suggest that $\delta < 0.02°$.) It is straightforward to show that ε is also insensitive to the other adopted constants required in C_1, C_2 and C_3.

Equation (2) is analogous to the simpler equation (8) of Zschau[1]. Zschau was able to write an additional equation for the in-phase component ($k_2 \cos\varepsilon$) and thereby estimated both k_2 and ε (at least in principle; in practice the ocean models available to him were too inaccurate for this). Here, because of our use of altimetry, we cannot estimate k_2 independently of h_2. Alternatively, we may use the in-phase components to place bounds on δ. This must be examined in more detail elsewhere, but the bounds turn out to be weak and, given the lack of any systematic in-phase difference in Fig. 1, the result is not significantly different from zero.

For the tidal coefficients D_{22}^{A}, ψ_{22}^{A}, D_{22}^{T}, ψ_{22}^{T}, we adopt the means of the appropriate models listed in Table 1. For the tracking and altimeter standard errors, we use 0.024 and 0.036 cm, respectively; the latter is simply the listed value for the one model and ignores averaging as all three altimeter models use essentially the same data. Solution of equation (2) then yields $\varepsilon = 0.16° \pm 0.09°$. This value of ε implies[13] that friction in the Earth's body tide consumes 83 ± 45 gigawatts of tidal power. For comparison, this is ~3% of the ocean's dissipation, and, according to Platzman's estimate[22], about eight times the atmosphere's dissipation. If Q^{-1} is the body tide's specific dissipation function, then the effective tidal $Q = 1/\tan\varepsilon$ is found to be 370, with approximate confidence limits of (200,800).

This estimate of Q helps fill an important observational gap between seismic modes of period less than 1 hour and the Chandler wobble of period 14 months; even measurements with relatively wide confidence bounds may help clarify previous disparate theoretical and/or indirect estimates. For example, one indirect approach[2] infers tidal Q from free-oscillation data, arguing that the body tide and the ${}_0S_2$ free-oscillation mode should, aside from a slight frequency dependence, display similar Q (although Bostrom[3] suggests that the Earth's rotation may reduce the tidal Q). Munk[4], in fact, adopted a free-oscillation Q of 350 (now thought to be too low[5]) to estimate a solid-Earth tidal dissipation essentially equivalent to our observational estimate. Other theoretical estimates of complex k_2 Love numbers[6] suggest bounds on tidal Q of (90, 500), with a preference around 210, whereas another[7] k_2 value suggests a Q of 126, which is outside our (1σ) observational range. Finally, Zschau[1], adopting a single absorption-band model between seismic and Chandler wobble periods, arrives at 'most probable' estimates for ε of 0.21° and solid-Earth dissipation of 120 GW. Within their error bounds, our observations are consistent with Zschau's values and with the assumed smooth frequency dependence between seismic and Chandler periods. □

Received 19 January; accepted 8 May 1996.

1. Zschau, J. in *Space Geodesy and Geodynamics* (eds Anderson, A. & Cazenave, A.) 315–344 (Academic, London, 1986).
2. Lagus, P. L. & Anderson, D. L. *Phys. Earth planet. Inter.* **1,** 505–510 (1968).
3. Bostrom, R. C. *EOS* **76,** F60 (1995).
4. Munk, W. *Q. Jl R. astr. Soc.* **9,** 352–375 (1968).
5. Tanimoto, T. *Geophys. Res. Lett.* **17,** 669–672 (1990).
6. Wahr, J. & Bergen, Z. *Geophys. J. R. astr. Soc.* **87,** 633–668 (1986).
7. Dehant, V. *Phys. Earth planet. Inter.* **49,** 97–116 (1987).
8. Lambeck, K. *Phil. Trans. R. Soc. Lond.* **A287,** 545–594 (1977).
9. Ray, R. D. in *The Oceans* (eds. Majumdar, S. K. *et al.*) 171–185 (Pennsylvania Academy of Science, Easton, 1994).
10. Fu, L.-L. *et al. J. geophys. Res.* **99,** 24369–24381 (1994).
11. Cohen, S. C. & Smith, D. E. *J. geophys. Res.* **90,** 9217–9220 (1985).
12. Munk, W. H. & MacDonald, G. J. F. *The Rotation of the Earth* (Cambridge Univ. Press, 1960).
13. Platzman, G. W. *Rev. Geophys. Space Phys.* **22,** 73–84 (1984).
14. Cartwright, D. E. & Ray, R. D. *J. geophys. Res.* **96,** 16897–16912 (1991).
15. Schrama, E. J. O. & Ray, R. D. *J. geophys. Res.* **99,** 24799–24808 (1994).
16. Marshall, J. A. *et al. J. geophys. Res.* **100,** 25331–25352 (1995).
17. Le Provost, C., Bennett, A. F. & Cartwright, D. E. *Science* **267,** 639–642 (1995).
18. Andersen, O. B., Woodworth, P. L. & Flather, R. A. *J. geophys. Res.* **100,** 25261–25282 (1995).
19. Lerch, F. *Bull. Géod.* **65,** 44–52 (1991).
20. Wunsch, C. & Stammer, D. *J. geophys. Res.* **100,** 24895–24910 (1995).
21. Haurwitz, B. & Cowley, A. D. *Pure appl. Geophys.* **102,** 193–222 (1973).
22. Platzman, G. W. *Pure Appl. Geophys.* **137,** 1–33 (1991).
23. Zschau, J. in *Tidal Friction and the Earth's Rotation* (eds Brosche, P. & Sündermann, J.) 62–94 (Springer, New York, 1978).
24. Pagiatakis, S. D. *Geophys. J. Int.* **103,** 541–560 (1990).
25. Ray, R. D., Sanchez, B. & Cartwright, D. E. *EOS* **75,** 108 (1994).
26. Eanes, R. J. *EOS* **75,** 108 (1994).
27. Lerch, F. J. *et al.* NASA Tech. Memo. 104555 (Goddard Space Flight Center, Greenbelt, 1992).
28. Tapley, B. D., Schutz, B. E., Eanes, R. J., Ries, J. C. & Watkins, M. M. in *Cotnributions of Space Geodesy to Geodynamics: Earth Dynamics* (eds Smith, D. E. & Turcotte, D.) 147–174 (Am. geophys. Union, Washington, 1993).
29. Gill, A. *Atmosphere-Ocean Dynamics* (Academic, New York, 1982).
30. Le Provost, C., Genco, M. L., Lyard, F., Vincent, P. & Canceil, P. *J. geophys. Res.* **99,** 24777–24797 (1994).
31. Schwiderski, E. W. *Mar. Geol.* **6,** 219–265 (1983).
32. Parke, M.E. & Hendershott, M. C. *Mar. Geol.* **3,** 379–407 (1980).

ACKNOWLEDGEMENTS. We thank C. F. Yoder and especially G. W. Platzman for useful discussions, and C. Wunsch for his frequency-wavenumber spectra.

CORRESPONDENCE should be addressed to R.D.R. (e-mail: ray@nemo.gsfc.nasa.gov).

The guinea-pig is not a rodent

Anna Maria D'Erchia*†, Carmela Gissi*†, Graziano Pesole‡, Cecilia Saccone*§ & Ulfur Arnason†

* Dipartimento di Biochimica e Biologia Molecolare, Università di Bari, 70125 Bari, Italy
† Department of Evolutionary Molecular Systematics, University of Lund, Sölvegatan 29, S-22362 Lund, Sweden
‡ Dipartimento di Biologia DBAF, Università della Basilicata, 30100 Potenza, Italy
§ Centro di Studio sui Mitocondri e Metabolismo Energetico, Consiglio Nazionale delle Ricerche, 70125 Bari, Italy

In 1991 Graur *et al.* raised the question of whether the guinea-pig, *Cavia porcellus*, is a rodent[1]. They suggested that the guinea-pig and myomorph rodents diverged before the separation between myomorph rodents and a lineage leading to primates and artiodactyls. Several findings have since been reported, both for and against this phylogeny, thereby highlighting the issue of the validity of molecular analysis in mammalian phylogeny. Here we present findings based on the sequence of the complete mitochondrial genome of the guinea-pig, which strongly contradict rodent monophyly. The conclusions are based on the cumulative evidence provided by orthologically inherited genes and the use of three different analytical methods, none of which joins the guinea-pig with myomorph rodents. In addition to the phylogenetic conclusions, we also draw attention to several factors that are important for the validity of phylogenetic analysis based on molecular data.

The order Rodentia is by far the most speciose mammalian order, comprising 1,814 species and 29 families. It is traditionally divided into three suborders: Sciuromorpha (squirrels), Myomorpha (mice, rats), and Hystricomorpha (porcupines, guinea-pigs).

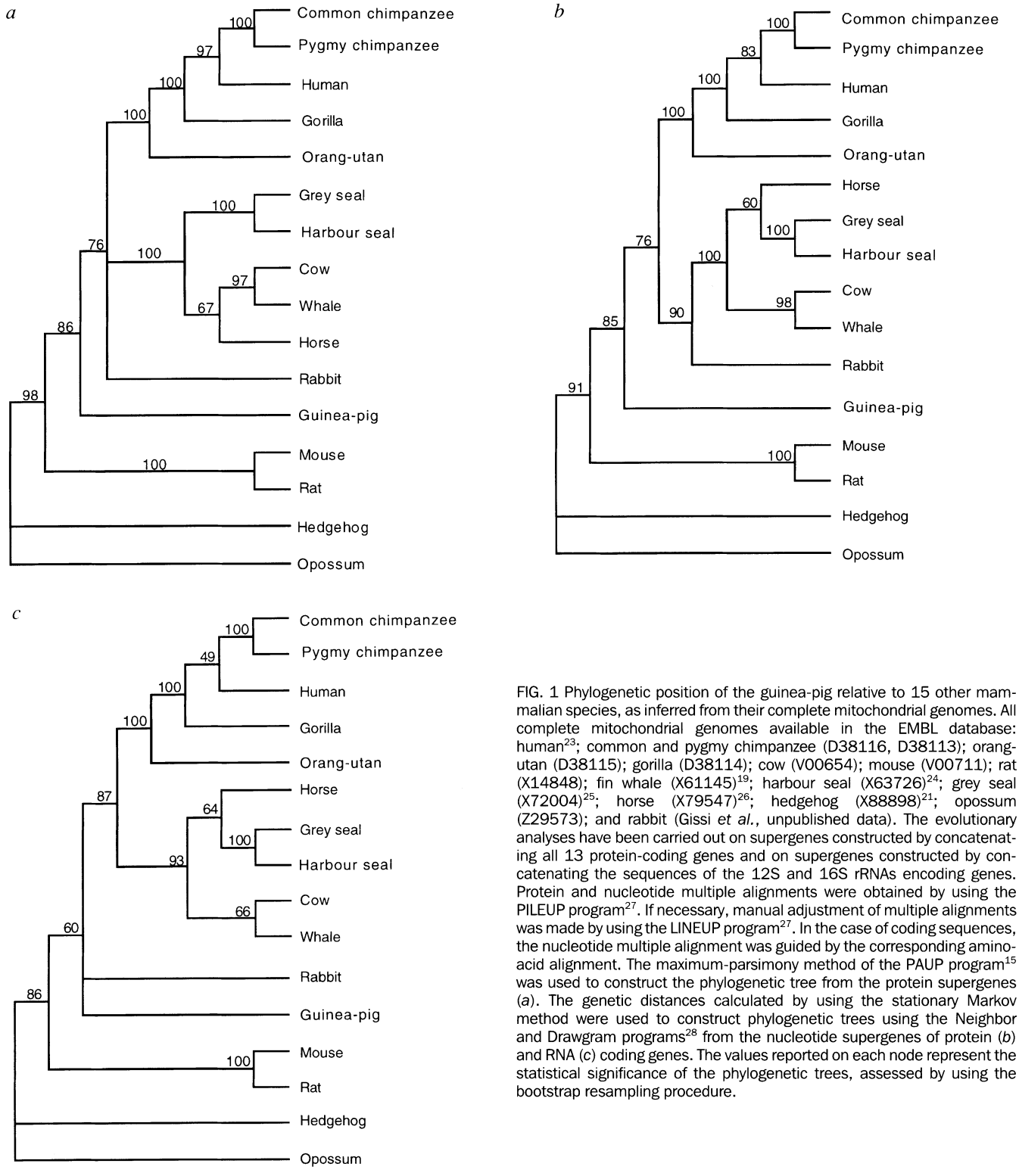

FIG. 1 Phylogenetic position of the guinea-pig relative to 15 other mammalian species, as inferred from their complete mitochondrial genomes. All complete mitochondrial genomes available in the EMBL database: human[23]; common and pygmy chimpanzee (D38116, D38113); orang-utan (D38115); gorilla (D38114); cow (V00654); mouse (V00711); rat (X14848); fin whale (X61145)[19]; harbour seal (X63726)[24]; grey seal (X72004)[25]; horse (X79547)[26]; hedgehog (X88898)[21]; opossum (Z29573); and rabbit (Gissi *et al.*, unpublished data). The evolutionary analyses have been carried out on supergenes constructed by concatenating all 13 protein-coding genes and on supergenes constructed by concatenating the sequences of the 12S and 16S rRNAs encoding genes. Protein and nucleotide multiple alignments were obtained by using the PILEUP program[27]. If necessary, manual adjustment of multiple alignments was made by using the LINEUP program[27]. In the case of coding sequences, the nucleotide multiple alignment was guided by the corresponding amino-acid alignment. The maximum-parsimony method of the PAUP program[15] was used to construct the phylogenetic tree from the protein supergenes (*a*). The genetic distances calculated by using the stationary Markov method were used to construct phylogenetic trees using the Neighbor and Drawgram programs[28] from the nucleotide supergenes of protein (*b*) and RNA (*c*) coding genes. The values reported on each node represent the statistical significance of the phylogenetic trees, assessed by using the bootstrap resampling procedure.

The guinea-pig, *Cavia porcellus*, is generally classified as a New World hystricomorph rodent belonging to the family Caviomorpha. The joining of the three rodent suborders into a single clade was supported by morphological data. This view had not been questioned until Graur *et al.*[1] concluded, on the basis of maximum parsimony analysis of 15 protein sequences, that the order Rodentia is polyphyletic, and suggested that the suborder Hystricomorpha should be separated from the Rodentia and given the status of an order, Hystricomorpha. The phylogenetic position of the guinea-pig relative to other rodents, and hence also rodent phylogeny in general, has since become a matter of considerable contention among evolutionists, and rodent monophyly has been questioned by analyses of other sets of nucleotide and protein sequences[2-6]. However, some of the former set of sequence data have been re-examined using the maximum-likelihood method[7,8], and 19 protein sequences using four groups of taxa[9], and sequences of mitochondrial 12S and 16S ribosomal RNA genes[10] have been analysed, all with inconclusive results. A different approach, based on studies of BC1 RNA expression, a retroposon element that is present in all rodents and guinea-pig but not in some other mammals, has again suggested rodent monophyly[11].

These inconsistent, and even contradictory, findings show that the evolutionary position of the guinea-pig has not been unequivocally clarified, although it cannot be excluded that some of the controversies may be due to the different analytical approaches used, insufficient number of taxa examined, or to the inadequate length of the sequences used in the phylogenetic analyses.

In an attempt to shed light on this problem, we have sequenced the complete mitochondrial genome (mtDNA) of the guinea-pig. We chose mtDNA because of its maternal inheritance, lack of recombination, and especially the presence of orthologous genes that make it a particularly suitable and powerful tool for phylogenetic analysis.

The study has included 14 complete mammalian mtDNA sequences available in the literature, representing eight acknowledged orders: Primates, Artiodactyla, Cetacea, Perissodactyla, Carnivora, Rodentia, Insectivora and Marsupialia (outgroup). We have also included mtDNA from the rabbit (Lagomorpha), the sequence of which was recently determined (C.G. *et al.*, unpublished results). On morphological grounds, the Lagomorpha is claimed to form a monophyletic clade with Rodentia (the so-called Glires)[12], but molecular data do not support this relationship[13,14]. The inclusion of Lagomorpha is therefore particularly relevant in this evolutionary analysis.

To minimize the methodological bias, we performed the phylogenetic analyses by using three completely different methods: (1) the maximum-parsimony method[15], a deterministic method that we applied to the derived protein sequences; (2) the protein maximum-likelihood method[16]; and (3) the stationary Markov model[17], a stochastic method that we applied to nucleotide sequences.

The phylogenetic tree (maximum parsimony analysis) based on the concatenated sequences of all 13 protein-coding mitochondrial genes is shown in Fig. 1*a*. A clade comprising Lagomorpha, Primates, Carnivora, Perissodactyla, Artiodactyla and Cetacea is supported by a bootstrap value of 76%. Consistent with previous findings there is a distinct affinity between Artiodactyla and Cetacea[18–21]. The position of Lagomorpha remains unsettled, as the low bootstrap value does not allow us to resolve the trichotomy among Lagomorpha, Primates and the clade including Carnivora, Perissodactyla, Artiodactyla and Cetacea. The guinea-pig falls outside the myomorph rodents (mouse, rat) as a sister-group of the clade including Lagomorpha, Primates, Carnivora, Perissodactyla, Artiodactyla and Cetacea. The alternative topology with a monophyletic Rodentia has a bootstrap support value of only 1%. Insectivora, represented by the hedgehog, *Erinaceus europaeus*, appears at the basal branch of the eutherian tree, consistent with previous results[21]. The analysis of protein supergenes using the maximum-likelihood method[16] results essentially in the same tree topology (data not shown), with Lagomorpha more closely related to the clade including Artiodactyla, Cetacea, Perissodactyla and Carnivora.

The phylogenetic tree obtained by applying the neighbour-joining method[22] on the pairwise distances of the concatenated nucleotide sequences of the 13 protein-coding genes, as calculated by applying the stationary Markov model on asynonymous nucleotide substitutions, is shown in Fig. 1*b*. Synonymous substitutions have not been included in the analysis because they show a marked compositional heterogeneity among mammals (lack of stationarity), and also, because of their fast substitution rate, the nucleotide divergence is well above the saturation level for many interspecies comparisons. The close relationship between the guinea-pig and the Lagomorpha/Primates/Carnivora/Perissodactyla/Artiodactyla(+Cetacea) clade is again supported by high bootstrap values (85%) (Fig. 1*b*), whereas the alternative tree with a monophyletic Rodentia has a bootstrap value of 10%.

The phylogenetic tree obtained by using the stationary Markov model/neighbour-joining method on the rRNA supergenes is shown in Fig. 1*c*. It reproduces results reported in Fig 1*a*, *b*, further supporting the phylogenetic relationships described above.

Our analyses of the phylogenetic position of the guinea-pig were performed using a comprehensive data set, both with respect to the number of orthologous genes and to the number of mammalian orders examined. The different analytical approaches and sets of data yielded congruent results that were consistent with the hypothesis of Rodent polyphyly[1]. It should be noted, however, that our trees, which identify the guinea-pig as an outgroup to Lagomorpha/Primates/Carnivora/Perissodactyla/Artiodactyla(+Cetacea), differ slightly from that proposed by Graur *et al.*, in which the guinea pig constitute an outgroup to myomorph rodents, primates and artiodactyls[1].

Phylogenetic relationships among Rodentia (*sensu lato*) have been addressed by analysing nuclear[9] and mitochondrial rRNA genes[10]. Regarding the analysis of nuclear genes[9], it is worth noting that, although the findings, in general, do not support rodent polyphyly, different genes have provided dissimilar answers to the question of rodent phylogeny. Such discrepancies are often observed when using nuclear genes, perhaps because some genes evolve under different evolutionary constraints in the various tree branches, or because the genes analysed might be paralogous. In contrast, mitochondrial genomes contain only orthologous single-copy genes, and can thus provide more reliable phylogenies.

Our results obtained with mt rRNA (Fig. 1*c*), which confirm the findings based on protein-coding genes, are inconsistent with previous findings[10] that support rodent monophyly by analysing these same genes. These differences might be due to differences in the multiple alignment, which in the case of rRNA genes is not obvious, rather than to the analytical approach applied.

The close relationship we found between Cetacea and Artiodactyla is strongly supported, confirming previous molecular data[18–21]. The positions of Perissodactyla and Lagomorpha remain uncertain, but a clade including Cetacea, Artiodactyla, Carnivora and Perissodactyla is strongly supported. Our data contradict morphological studies[12] that place Rodentia and Lagomorpha in the monophyletic cohort Glires, but agree with other molecular evolutionary analyses based on nuclear encoded proteins[14] that place Lagomorpha closer to Primates than to Rodentia; both analyses reject the monophyletic Glires. The stationary Markov model/neighbour-joining and the protein maximum-likelihood findings, which place Lagomorpha closely akin to the clade including Artiodactyla, Cetacea, Perissodactyla and Carnivora, are highly suggestive, but more data are necessary before this relation can be considered reliable.

The phylogenetic position of the guinea-pig is highly reliable, as different methodological approaches provide highly consistent results. The large number of sites included, and the very significant bootstrap values obtained, provide strong evidence in favour of the inclusion of guinea-pig in a new mammalian order distinct from Rodentia.

Because of the exceptional complexity of the order Rodentia, sequence data are still limited, and the phylogeny will be clearer when a larger number of species can be considered in phylogenetic analyses. □

Received 9 November 1995; accepted 8 May 1996.

1. Graur, D., Hide, W. A. & Li, W. H. *Nature* **351,** 649–652 (1991).
2. Li, W. H., Hide, W. A., Zharkikh, A., Ma, D. P. & Graur, D. *J. Heredity* **83,** 174–181 (1992).
3. Graur, D., Hide, W. A., Zharkirkh, A. & Li, W. H. *Comp. Biochem. Physiol.* **101B,** 495–498 (1992).
4. Wolf, B., Reinecke, K., Aumann, K. D., Brigelius-Flohè, R. & Flohè, L. *Biol. Chem. Hoppe-Seyler* **374,** 641–649 (1993).
5. Noguchi, T., Fujiwara, S., Hayashi, S. & Sakuraba, H. *Comp. Biochem. Physiol.* **107,** 179–182 (1994).
6. Ma, D. P., Zharkikh, A., Graur, D., VandeBerg, J. L. & Li, W. H. *J. molec. Evol.* **36,** 327–334 (1993).
7. Hasegawa, M., Cao, Y., Adachi, J. & Yano, T. *Nature* **355,** 595 (1992).
8. Cao, Y., Adachi, J., Yano, T. & Hasegawa, M. *Molec. Biol. Evol.* **11,** 593–604 (1994).
9. Kuma, K. & Miyata, T. *Jap. J. Genet.* **69,** 555–566 (1994).
10. Frye, M. S. & Hedges, S. B. *Molec. Biol. Evol.* **12(1),** 168–176 (1995).
11. Martignetti, J. A. & Brosius, J. *Proc. natn. Acad. Sci. U.S.A.* **90,** 9698–9702 (1993).
12. Novacek, N. J. *Nature* **356,** 121–125 (1992).
13. Graur, D. *FEBS Lett.* **325,** 152–159 (1993).
14. Graur, D., Duret, L. & Gouy, M. *Nature* **379,** 333–335 (1996).
15. Swofford, D. L. *PAUP: Phylogenetic Analysis Using Parsimony* Version 3.1.1 (Illinois Natural History Survey, Champaign, 1993).

16. Adachi, J. & Hasegawa, M. *MOLPHY: Programs for Molecular Phylogenetics 2.2* (Computer Science Monographs, No. 27, Institute of Statistical Mathematics, Tokyo, 1992).
17. Saccone, C., Lanave, C., Pesole, G. & Preparata, G. *Meth. Enzym.* **183,** 570–583 (1990).
18. Irwin, D. M., Kocher, T. D. & Wilson, A. C. *J. molec. Evol.* **32,** 128–144 (1991).
19. Arnason, U., Gullberg, A. & Widegren, B. *J. molec. Evol.* **33,** 556–568 (1991).
20. Graur, D. & Higgins, D. G. *Molec. Biol. Evol.* **11,** 357–364 (1994).
21. Krettek, A., Gullberg, A. & Arnason, U. *J. molec. Evol.* **41,** 952–957 (1995).
22. Saitou, N. & Nei, M. *Molec. Biol. Evol.* **4,** 406–425 (1987).
23. Arnason, U., Xu, X. & Gullberg, A. *J. molec. Evol.* **42,** 145–152 (1996).
24. Arnason, U. & Johnsson, E. *J. molec. Evol.* **34,** 493–505 (1992).
25. Arnason, U., Gullberg, A., Johnsson, E. & Ledje, C. *J. molec. Evol.* **37,** 323–330 (1993).
26. Xu, X. & Arnason, U. *Gene* **148,** 357–362 (1994).
27. Devereux, J., Haeberli, P. & Smithies, O. *Nucleic Acids Res.* **12,** 387–395 (1984).
28. Felsestein, J. *PHYLIP (Phylogeny Inference Package), Version 3.5c* (University of Washington, Seattle, 1993).

ACKNOWLEDGEMENTS. This work was supported by MURST (Italy), the Swedish Natural Sciences Research Council, and an EEC grant.

CORRESPONDENCE and requests for materials should be addressed to C.S. (e-mail: saccone@area.ba.cnr.it). Protein and nucleotide alignments analysed in the study are available on the World-Wide Web at http://www.ba.cnr.it/guineapig.html.

FIG. 1 *A*, Faroe Islands; *B*, Bornholm; *C*, Reykjavik (scaled). These are all ▶ examples of Bartlett's type III measles epidemic dynamics[12]. Top, monthly measles-case returns for each of the three communities. Between 1920 and 1970 the population of Reykjavik grew from 20,000 to 100,000, so we have scaled the incidence data per 25,000 of population. Middle, the distribution of epidemic event sizes. For the Faroes, $b \simeq 0.28$; for Bornholm, $b \simeq 0.28$; and for Reykjavik, $b \simeq 0.21$. Bottom, distribution of epidemic event durations. For the Faroe Island data, $c \simeq 0.8$; for Bornholm, $c \simeq 0.85$; and for Reykjavik, $c \simeq 0.62$. Clearly, scaling the measles incidence data will affect the epidemic sizes but leave the epidemic durations unscaled, hence this exponent is somewhat different from the Faroe and Bornholm cases. For each population, the exponents are unaffected by the specific choice of binning by decade.

Power laws governing epidemics in isolated populations

C. J. Rhodes & R. M. Anderson

Centre for the Epidemiology of Infectious Disease, Department of Zoology, University of Oxford, South Parks Road, Oxford OX1 3PS, UK

TEMPORAL changes in the incidence of measles virus infection within large urban communities in the developed world have been the focus of much discussion in the context of the identification and analysis of nonlinear and chaotic patterns in biological time series[1–11]. In contrast, the measles records for small isolated island populations are highly irregular, because of frequent fade-outs of infection[12–14], and traditional analysis[15] does not yield useful insight. Here we use measurements of the distribution of epidemic sizes and duration to show that regularities in the dynamics of such systems do become apparent. Specifically, these biological systems are characterized by well-defined power laws in a manner reminiscent of other nonlinear, spatially extended dynamical systems in the physical sciences[16–19]. We further show that the observed power-law exponents are well described by a simple lattice-based model which reflects the social interaction between individual hosts.

Isolated island populations have often provided a valuable arena for the study of evolutionary and ecological processes because the subject of investigation is confined to a well-defined region of space that is well insulated from the influence of external factors. In the context of population studies, it is often possible in such settings to better observe effects that are intrinsic to the community without having to quantify the effect of peripheral populations.

The Faroe Islands (population 25,000) have extensive detailed measles-case returns (Fig. 1*A*, top). It is considered to be an accurate epidemiological data set because the population is small and localized. Also, because of the comparative rarity of measles outbreaks, few measles cases escape notice[20]. In the 58-year interval, there are 43 distinct epidemic events. An epidemic event is defined as the presence of a finite number of cases recorded in a sequence of consecutive months bounded by an absence of cases. An epidemic event has a duration, t, where $t = \tau_{end} - \tau_{start}$, τ_{start} is the month when cases in an event first appear, and τ_{end} is the next month when there are no more cases present. Similarly, an epidemic event has a size, s, where $s = \sum_{\tau_{start}}^{\tau_{end}} C(\tau)$, and $C(\tau)$ is the number of recorded cases of measles in the month τ.

From Fig. 1*A*, top, it is apparent that there is no obvious discernible pattern to the dynamics; there is wide variation in both the duration and size of the epidemic events, reminiscent of the sort of dynamics observed in the study of earthquakes. In that case, the Gutenberg–Richter[21] law acts as an organizing principle connecting the frequency and magnitude of larger and smaller earthquakes. Performing the same analysis here, counting the number of epidemic events of size $>s$, there is a power-law dependence of the form $\log N(>s) = a - b\log(s)$. Thus, the number of epidemic events of size s scales as $N(s) \propto s^{-1-b}$, where $b \simeq 0.28$. The same analysis for the epidemic event durations indicates that the number of epidemics of duration t scales as $N(t) \propto t^{-1-c}$, where, from Fig. 1*A*, bottom, $c \simeq 0.8$. The presence of these scaling relations provides a useful way of estimating the likelihood, in a given interval of time, of epidemics of size s and duration t. Small short epidemics occur more often than large long epidemics, although their occurrence is connected and governed by the scaling exponents b and c. The exponents also apply to subportions of the data so, for example, we can use the epidemic distribution measured from the first half of the data set to predict the likely distribution of epidemic events in the second half.

We have also applied this analysis to two other subendemic populations with extensive and accurate measles records, Bornholm and Reykjavik. Figure 1*B*, *C* indicates that the exponents, b and c, for all three populations are remarkably similar.

Mechanisms leading to the emergence of power laws of this sort are still not fully understood, although recently many spatially extended interacting model systems have been shown to exhibit similar behaviour. We use one such lattice-based model, previously used in discussion of 'forest-fire' dynamics[18,22,23], to provide a simple model for this phenomenon.

The dynamics of the model in Fig. 2 closely resemble those seen in the Faroe data. Exponents for the model data are similar to the actual epidemiological data; $b \simeq 0.29$ and $c \simeq 1.5$, with the simulation underestimating the number of long epidemics of more than 10 months duration. The connectedness of the spatial distribution of the population on the lattice seems to reflect the social networks that exist in real communities[24].

FIG. 2 Top left, time series of infectives for the model simulation. Each site in the $L \times L$ lattice is in one of three states: empty, occupied by a susceptible, or occupied by an infective. The lattice is updated synchronously at each time-step using the following rules: (1) susceptibles who are on nearest-neighbour sites to an infective become infective themselves; (2) infectives become inactive and the site they occupy becomes empty; (3) susceptibles are introduced onto empty lattice sites with a probability μ; (4) a new infective can arise when a susceptible is spontaneously infected with a probability ν. This effectively corresponds to an immigration term, whereby our lattice population is subject to infrequent infection from external sources. Periodic boundary conditions are used. These rules define a simple spatial *S-I* model. It is the simplest possible model of epidemic spread on a lattice and is, at best, a caricature of the known epidemiological processes. The lattice is 250 × 250, with $\mu = 0.000026$ and $\nu = \mu/300$.